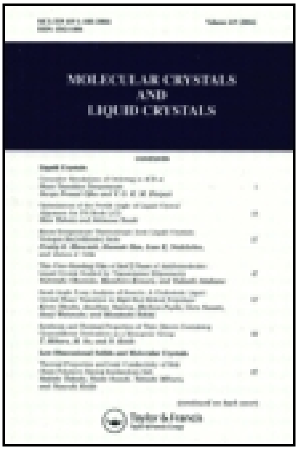

Molecular Crystals and Liquid Crystals Science and Technology. Section A. Molecular Crystals and Liquid Crystals
Publication details, including instructions for authors and subscription information:
http://www.tandfonline.com/loi/gmcl19

The Character of Photochemical Conversions of 2,3-Substituted-1,4-Naphthoquinones in Solution from the Standpoint of their Molecular and Crystal Structure

S. M. Aldoshin [a] , I. I. Chuev [a] , O. S. Filiponko [a] , M. A. Novozhilova [a] & V. S. Nedzvetski [a]

[a] Institute of Chemical Physics in Chemogolovka, Russian Acad. Sci., Chernogolovka, Moscow r-n, 142432, Russia

Version of record first published: 24 Sep 2006.

To cite this article: S. M. Aldoshin , I. I. Chuev , O. S. Filiponko , M. A. Novozhilova & V. S. Nedzvetski (1993): The Character of Photochemical Conversions of 2,3-Substituted-1,4-Naphthoquinones in Solution from the Standpoint of their Molecular and Crystal Structure, Molecular Crystals and Liquid Crystals Science and Technology. Section A. Molecular Crystals and Liquid Crystals, 231:1, 231-251

To link to this article: http://dx.doi.org/10.1080/10587259308032509

Mol. Cryst. Liq. Cryst., 1993, Vol. 231, pp. 231–251
Reprints available directly from the publisher
Photocopying permitted by license only

Printed in the United States of America

The Character of Photochemical Conversions of 2,3-Substituted-1,4-Naphthoquinones in Solution from the Standpoint of their Molecular and Crystal Structure

S. M. ALDOSHIN, I. I. CHUEV, O. S. FILIPONKO, M. A. NOVOZHILOVA and V. S. NEDZVETSKI

Institute of Chemical Physics in Chernogolovka, Russian Acad. Sci., Chernogolovka, Moscow r-n, 142432, Russia

(Received July 6, 1992)

An X-ray analysis of 2,3-substituted-1,4-naphthoquinones has been performed. On the basis of obtained data the structure factors causing the photoactivity of the investigated compounds has been determined. The study of photochemistry of these compounds in ethanol in common with quantum-chemical calculations (INDO/S, MNDO) has made it possible to suggest a mechanism of photoconversion for these compounds in solution connected with hydrogen atoms elimination and further synchronous cycle closure.

INTRODUCTION

Earlier it was reported[1] that UV-initiated photochemical transformations of 2,3-derivatives of 1,4-naphthoquinones I in solution were connected with an elimination of a hydrogen atom followed by a five-member cycle closure (Scheme I). Photoproduct *P* formed here was further readily hydrogenized with elimination of a CHR group.

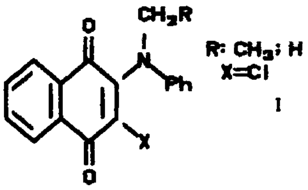

I

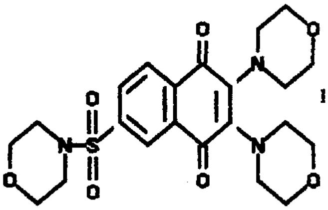

II

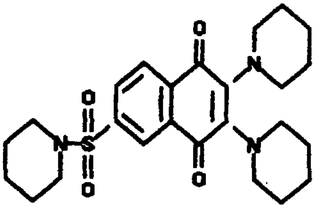

III

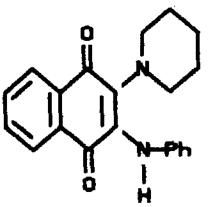

IV

An X-ray study of the close by structure derivatives of 4a,5,8,8a-tetrahydro-1,4-naphthoquinones and some photoproducts formed in the solid state and/or in solutions carried out by J. Trotter and others$^{2-4}$ made it possible to establish the dependence of the character of solid-phase photoconversions in these compounds on their crystal structure.

The primary act of the photoreactions studied in the above works is a β-H or γ-H elimination of a hydrogen atom. An H ··· O distance in these compounds is in the range of 2.3 ÷ 2.6 Å which is considerably less than the sum of Van-der-Waals radii of atoms H and O, 2.72 Å. Angles τ_0, Δ_0 and θ_0 are close to the ideal direction of a hydrogen atom onto a lone electron pair of a carbonyl oxygen atom in the case of a β-H atom elimination or onto a carbon atom p_Z-orbital when a γ-H atom is eliminated[3] (Scheme II).

To study the peculiarities of the molecular structure and its influence on the character of photoconversions for 2,3-substituted-1,4-naphthoquinones II–IV we have carried out X-ray investigations of their crystals and a spectral study in solutions.

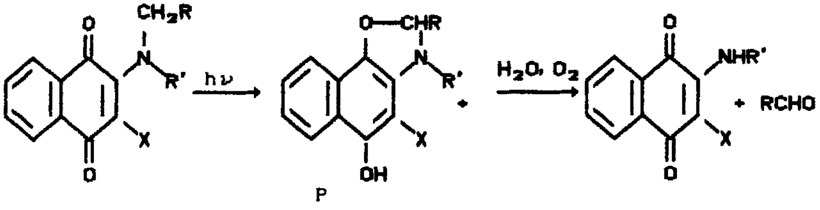

SCHEME I

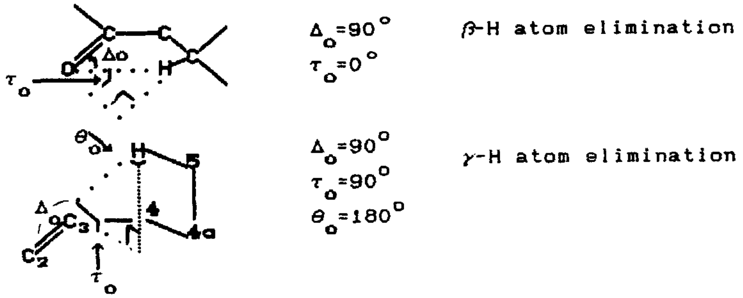

SCHEME II Structural parameters determining the elimination of β-H and γ-H atoms in tetrahydronaphthoquinones.

EXPERIMENTAL

Compounds II–IV crystallize as black needles, crystals of monoclinic syngony. The main crystal data are listed in the Table:

Compound	Space group	a, Å	b, Å	c, Å	γ,°	d, g/cm^3
II	P21/b	13.750(6)	15.400(3)	12.165(4)	60.90(1)	1.418
III	P21/b	12.581(7)	20.227(5)	9.655(9)	97.90(1)	1.294
IV	P21/b	6.255(7)	17.136(5)	16.017(9)	81.00(1)	1.305

A set of experimental reflections was obtained on a DAR-UM difractometer, CuK$_\alpha$-radiation. The data are given in the Table:

Compound	Number ref I > 3σ	Experimental region		Dimension of crystal, mm	R-factor
		θ min°	θ max°		
II	2393	1.6	32.8	.7 × .04 × .03	0.074
III	2434	1.8	31.8	.6 × .10 × .20	0.043
IV	1656	1.8	32.2	.6 × .20 × .30	0.062

The structures were solved by the direct method by the "Rentgen-75" program complex and refined by the full-matrix least-square method in anisotropic approximation. Hydrogen atoms were found from the difference Fourier synthesis and only positional parameters were refined for them. The atoms coordinates for compounds II–IV are given in Tables I–III, respectively.

TABLE I

Coordinates of non hydrogen atoms (×10^4) and hydrogen atoms (×10^3) in molecule II

Atom	X	Y	Z
S	2853(1)	4433(1)	3062(1)
O^{1}	5735(3)	6450(3)	921(4)
O^{2}	6929(4)	2623(3)	1285(5)
O^{3}	3194(4)	3413(3)	2859(5)
O^{4}	1746(3)	5173(2)	2846(4)
O^{5}	8931(4)	6283(2)	1120(4)
O^{6}	9980(3)	1322(3)	- 598(4)
O^{7}	3819(4)	4852(3)	6402(4)
N^{1}	7953(4)	5099(3)	618(4)
N^{2}	8527(3)	3050(3)	554(4)
N^{3}	3086(3)	4530(3)	4371(5)
C^{1}	6041(4)	5555(3)	989(5)
C^{2}	7184(4)	4789(2)	800(5)
C^{3}	7503(4)	3787(2)	866(5)
C^{4}	6690(3)	3492(2)	1263(5)
C^{5}	5541(3)	4272(2)	1566(5)
C^{6}	4819(3)	3999(2)	2044(4)
C^{7}	3759(3)	4727(3)	2345(4)
C^{8}	3414(3)	5734(3)	2130(4)
C^{9}	4144(3)	5985(3)	1623(4)
C^{10}	5216(4)	5273(2)	1374(4)
C^{11}	7796(4)	5919(3)	- 92(4)
C^{12}	7896(3)	6697(3)	591(4)
C^{13}	9061(3)	5502(3)	1861(4)

TABLE I (*continued*)

C^{14}	8995(3)	4691(3)	1187(4)
C^{15}	9053(3)	3110(3)	- 440(4)
C^{16}	9287(3)	2227(3)	-1171(4)
C^{17}	9451(3)	1252(3)	377(4)
C^{18}	9200(4)	2115(3)	1119(5)
C^{19}	2719(3)	5539(3)	4772(5)
C^{20}	2747(3)	5520(3)	6026(4)
C^{21}	4154(3)	3877(3)	6050(4)
C^{22}	4180(3)	3828(3)	4774(4)
H^{6}	514(3)	329(3)	224(5)
H^{8}	255(4)	624(4)	213(5)
H^{9}	386(4)	675(3)	136(5)
$H^{11.1}$	697(4)	623(3)	- 24(5)
$H^{11.2}$	830(4)	570(3)	- 82(5)
$H^{12.1}$	784(5)	724(3)	20(4)
$H^{12.2}$	704(4)	709(4)	96(5)
$H^{13.1}$	841(5)	577(3)	238(5)
$H^{13.2}$	986(5)	522(3)	232(5)
$H^{14.1}$	962(4)	439(4)	57(5)
$H^{14.2}$	904(4)	426(3)	190(5)
$H^{15.1}$	989(4)	308(3)	- 29(5)
$H^{15.2}$	878(5)	365(3)	- 87(5)
$H^{16.1}$	853(5)	223(3)	- 138(5)
$H^{16.2}$	978(5)	218(3)	- 172(5)
$H^{17.1}$	872(4)	120(4)	18(4)
$H^{17.2}$	1003(4)	56(4)	81(4)
$H^{18.1}$	878(4)	210(4)	182(5)
$H^{18.2}$	994(4)	212(4)	121(5)
$H^{19.1}$	197(4)	602(4)	465(5)
$H^{19.2}$	333(4)	571(4)	442(5)
$H^{20.1}$	247(5)	525(4)	637(5)
$H^{20.2}$	232(4)	633(4)	617(5)
$H^{21.1}$	496(4)	344(4)	634(5)
$H^{21.2}$	356(4)	364(4)	636(5)
$H^{22.1}$	441(4)	319(4)	448(5)
$H^{22.2}$	464(4)	403(4)	461(5)

TABLE II

Coordinates of non hydrogen atoms ($\times 10^4$) and hydrogen atoms ($\times 10^9$) in molecule III

Atom	X	Y	Z
S	2490(1)	470(1)	5287(1)
O^{1}	-1563(3)	- 780(2)	9408(3)
O^{2}	60(3)	-1882(2)	5045(4)
O^{3}	2487(3)	1174(2)	5388(4)
O^{4}	2568(3)	172(2)	3963(3)
N^{1}	-2561(3)	-2042(2)	8659(4)
N^{2}	-1666(3)	-2606(2)	6241(4)
N^{3}	3497(3)	290(2)	6213(4)
C^{1}	-1206(3)	-1039(2)	8391(5)
C^{2}	-1653(3)	-1709(2)	7947(5)
C^{3}	-1294(3)	-1983(2)	6747(5)
C^{4}	- 378(3)	-1618(2)	5970(5)
C^{5}	67(3)	- 927(2)	6401(4)
C^{6}	902(3)	- 575(2)	5657(4)
C^{7}	1331(3)	60(2)	6095(5)
C^{8}	929(3)	345(2)	7280(5)
C^{9}			

TABLE II (*continued*)

C	95(4)	- 15(2)	8003(4)
C^{10}	- 329(3)	- 655(2)	7575(4)
C^{11}	-1971(4)	-2704(2)	4794(5)
C^{12}	-1578(5)	-3330(3)	4212(6)
C^{13}	-2002(5)	-3940(3)	5102(7)
C^{14}	-1711(5)	-3803(3)	6581(7)
C^{15}	-2095(5)	-3168(2)	7133(6)
C^{16}	-3566(4)	-1790(3)	8391(6)
C^{17}	-4504(4)	-2301(3)	8805(6)
C^{18}	-4425(4)	-2477(3)	10325(5)
C^{19}	-3356(5)	-2696(3)	10613(6)
C^{20}	-2423(4)	-2177(3)	10136(6)
C^{21}	3738(4)	666(2)	7526(5)
C^{22}	4878(4)	598(3)	7928(5)
C^{23}	5035(4)	- 126(3)	8109(5)
C^{24}	4712(4)	- 512(2)	6780(5)
C^{25}	3596(3)	- 430(2)	6353(5)
H^{6}	122(4)	- 77(2)	478(5)
H^{8}	124(4)	85(3)	769(6)
H^{9}	- 309(4)	18(3)	887(6)
$H^{11.1}$	- 294(5)	- 279(3)	481(7)
$H^{11.2}$	- 162(4)	- 222(3)	421(6)
$H^{12.1}$	- 55(6)	- 321(3)	430(8)
$H^{12.2}$	- 179(5)	- 336(3)	318(7)
$H^{13.1}$	- 288(6)	- 409(3)	506(8)
$H^{13.2}$	- 245(5)	- 440(3)	471(7)
$H^{14.1}$	- 188(5)	- 415(3)	725(7)
$H^{14.2}$	- 84(5)	- 364(3)	660(7)
$H^{15.1}$	- 300(6)	- 325(4)	715(9)
$H^{15.2}$	- 168(5)	- 309(4)	807(8)
$H^{16.1}$	- 342(5)	- 123(3)	889(7)
$H^{16.2}$	- 351(4)	- 169(3)	727(7)
$H^{17.1}$	- 519(6)	- 207(4)	868(9)
$H^{17.2}$	- 445(6)	- 279(4)	822(8)
$H^{18.1}$	- 516(5)	- 286(3)	1059(7)
$H^{18.2}$	- 442(5)	- 208(3)	1092(7)
$H^{19.1}$	- 314(6)	- 311(3)	1007(8)
$H^{19.2}$	- 313(6)	- 280(3)	1167(8)
$H^{20.1}$	- 158(6)	- 233(4)	1021(9)
$H^{20.2}$	- 252(6)	- 179(4)	1075(8)
$H^{21.1}$	327(4)	44(3)	825(6)
$H^{21.2}$	355(5)	119(3)	745(7)
$H^{22.1}$	544(5)	79(3)	710(7)
$H^{22.2}$	507(5)	84(3)	872(8)
$H^{23.1}$	589(5)	- 16(3)	827(7)
$H^{23.2}$	461(5)	- 30(3)	886(7)
$H^{24.1}$	524(4)	- 32(3)	601(6)
$H^{24.2}$	479(4)	- 103(2)	691(6)
$H^{25.1}$	335(5)	- 62(3)	550(7)
$H^{25.2}$	295(5)	- 64(3)	705(7)

TABLE III

Coordinates of non hydrogen atoms ($\times 10^4$) and hydrogen atoms ($\times 10^3$) in molecule IV

Atom	X	Y	Z
O^1	2221(3)	5460(1)	4733(1)
O^2	6498(3)	5270(1)	1864(1)
N^1	1353(3)	4353(1)	3690(1)
N^2	3576(3)	4252(1)	2067(1)
C^1	3267(4)	5393(2)	4085(2)
C^2	2952(4)	4798(1)	3461(2)
C^3	4017(4)	4724(1)	2705(2)

TABLE III (*continued*)

C^{4}	5691(4)	5247(2)	2551(2)
C^{5}	6233(4)	5773(2)	3218(2)
C^{6}	7953(5)	6197(2)	3096(2)
C^{7}	8373(5)	6730(2)	3700(2)
C^{8}	7120(6)	6848(2)	4405(2)
C^{9}	5448(5)	6430(2)	4520(2)
C^{10}	5008(4)	5883(2)	3937(2)
C^{11}	1485(4)	3537(2)	3605(2)
C^{12}	- 377(4)	3202(2)	3751(2)
C^{13}	- 295(5)	2403(2)	3711(2)
C^{14}	1586(6)	1911(2)	3513(2)
C^{15}	3444(5)	2238(2)	3351(2)
C^{16}	3400(4)	3042(2)	3399(2)
C^{17}	1383(4)	4183(2)	1809(2)
C^{18}	1092(5)	4413(2)	896(2)
C^{19}	2756(6)	3914(2)	341(2)
C^{20}	5028(5)	3985(2)	645(2)
C^{21}	5265(5)	3772(2)	1562(2)
H^{N1}	74(4)	451(2)	415(2)
H^{6}	876(4)	611(2)	259(2)
H^{7}	951(4)	706(2)	361(2)
H^{8}	732(4)	726(2)	485(2)
H^{9}	461(4)	654(2)	504(2)
H^{12}	- 176(4)	356(2)	387(2)
H^{13}	- 165(4)	217(2)	383(2)
H^{14}	185(4)	137(2)	351(2)
H^{15}	495(4)	189(2)	319(2)
H^{16}	478(4)	329(2)	332(2)
$H^{17.1}$	124(4)	358(2)	186(2)
$H^{17.2}$	37(4)	454(2)	217(2)
$H^{18.1}$	- 37(4)	437(2)	74(2)
$H^{18.2}$	135(4)	3(2)	422(2)
$H^{19.1}$	259(4)	332(2)	40(2)
$H^{19.2}$	259(4)	413(2)	974(2)
$H^{20.1}$	609(4)	359(2)	32(2)
$H^{20.2}$	472(4)	43(2)	555(2)
$H^{21.1}$	509(4)	314(2)	162(2)
$H^{21.2}$	335(4)	113(2)	688(2)

Calculation of the energy of intermolecular interactions was made in the framework of atom-atomic approximations using "6-exp" potentials with parameters given in Reference 5.

Absorption spectra in ethanol were obtained on a "Specord UV-Visible" spectrophotometer. To carry out photochemical investigations a radiation source on the basis of a DRShch-250 lamp was used.

RESULTS AND DISCUSSION

1. Crystal Structure of Compound II

Molecule II is shown in Figure 1. The naphthoquinone fragment of molecule II is almost planar. The nonplanarity is caused mainly by the deviation of the oxygen

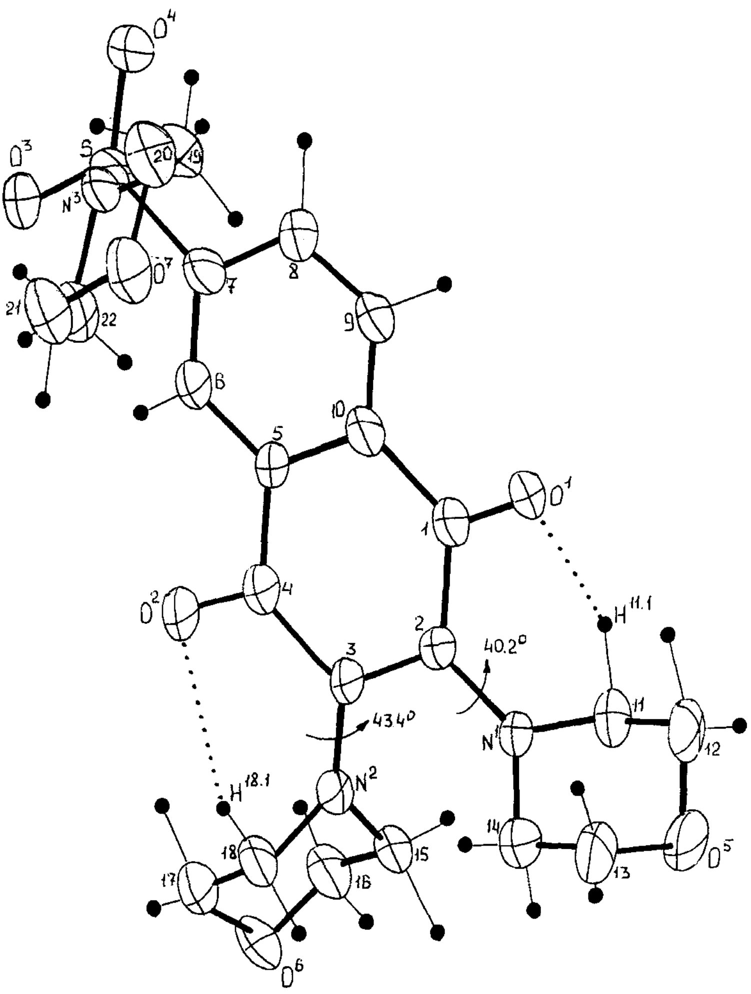

FIGURE 1 A general view of molecule II.

atoms of the carbonyl groups O^2 (-0.24 Å) and O^1 (0.10 Å) from the naphthoquinone plane to the opposite directions.

The orientation of the morpholine 2,3-substituents in the molecule is caused by a turning of the coordination planes of nitrogen atoms N^1 and N^2 with respect to the naphthoquinone plane by 40.2° and 43.4°, respectively. The nitrogen atoms N^2 and N^1 in the morpholine cycles have planar-trigonal coordination that favours the ($n_N\pi^*$) interaction and, hence, leads to shortening of the C$_3$—N^2 bond down to 1.364(5) Å and the C^2—N^1 bond down to 1.374(8) Å as compared with the standard values of the C—N bond length (1.47 Å).

Further increasing of the planarity in the structure is hindered by steric repulsions of the C^{14} $\cdots$ C^{15} carbon atoms, that belong to different morpholine substituents, with the contact between the atoms of 3.30 Å. These repulsions lead evidently to the nitrogen atoms N^2 and N^1 going out of the naphthoquinone fragment average plane by -0.09 and 0.41 Å, respectively.

Both the morpholine substituents have a "chair" conformation with twist angles along the C^{15} $\cdots$ C^{18} and C^{16} $\cdots$ C^{17} lines of 51.4° and 54.5° and along the C^{11} $\cdots$ C^{14} and C^{12} $\cdots$ C^{13} lines of 51.9° and 55.6°, respectively.

Bond length and angles in the morpholinosulfonyl fragments have ordinary values. The morpholine fragment has a "chair" conformation with twist angles along the C^{19} $\cdots$ C^{22} and C^{20} $\cdots$ C^{21} of 55.3° and 52.3°, respectively. The nitrogen atom N^3 in the cycle has a pyramidal coordination and is 0.34 Å out of the plane.

Crystal packing of II is shown in Figure 2. Molecules II in the crystal form irregular stacks oriented along the "c" direction where molecules are overlapped with the planar naphthoquinone fragments. The energies of the intermolecular interactions energy (IMIE) in the stack are different and equal to -17.5 and -13.7 kcal/mol. The IMIE between the molecules of the neighbouring stacks related with the glide plane along "b" is -6.0 kcal/mol.

With such a conformation in molecule II, shortened intramolecular contacts O^2 $\cdots$ H$^{18.1}$ (2.35 Å) and O^1 $\cdots$ H$^{11.1}$ (2.10 Å) are formed. Angles $C^4O^2H^{18.1}$ and $C^1O^1H^{11.1}$ at the carbonyl oxygen atoms are 93.0° and 93.1°. Hydrogen atoms H$^{18.1}$ and H$^{11.1}$ are 1.43 and 1.01 Å out of the carbonyl group planes. Analyzing, by Trotter,[3] the possibility of elimination of hydrogen atoms H$^{18.1}$ and H$^{11.1}$ we have calculated the corresponding structural parameters (Table IV). The data obtained are close to analogous values indicative of γ-H abstraction, that, in our case, testify for a possibility of a H$^{18.1}$ and H$^{11.1}$ atom elimination by a p_Z-orbital of the oxygen carbonyl atoms O^1 and O^2.

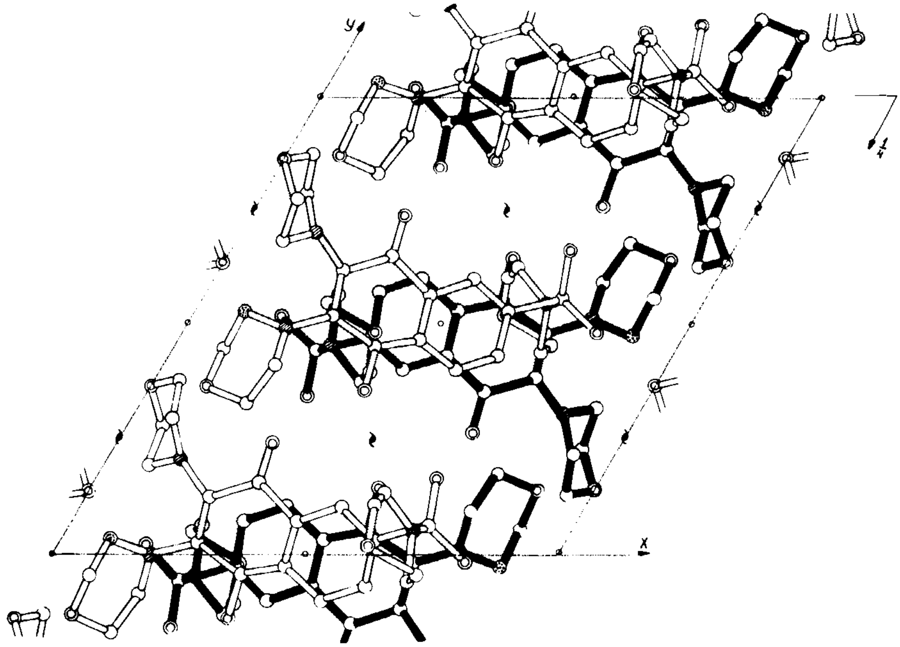

FIGURE 2 Projection of a crystal packing of molecules II on the XYO plane.

TABLE IV

Trotter structural parameters characterizing the hydrogen elimination

Compound	R, Å	τ, °	Δ, °	θ, °
II	2.35 2.10	37.5 28.75	93.1 93.0	106.7 107.0
III	2.44 2.27 2.57	38.2 48.5 20.0	103.0 86.0 94.0	109.2 110.2 107.9
IV	2.38	42.2	85.3	104.0
βH [2÷4]	2.46–2.72	0–8	80.7–86.4	85–93
γH [2÷4]	2.66–2.92	49.5–54.1	72.6–79.7	101–122

2. Crystal Structure of Compound III

The general view of molecule III is given in Figure 3. Similar to that in II, oxygen atoms O^1 and O^2 of the carbonyl groups deviate from the naphthoquinone plane by -0.02 and 0.18 Å, respectively.

The orientation of the piperidine 2,3-substituents towards the naphthoquinone fragment differs significantly from that of the morpholine substituents in II. The dihedral angles between the coordination planes of the nitrogen atoms N^2 and N^1 and the naphthoquinone plane are 40.8° and 82.6°, respectively. As distinct from II, the nitrogen atoms N^1 and N^2 have a pyramidal coordination, the deviation of the nitrogen atoms from the coordination plane being 0.34 and 0.13 Å, respectively.

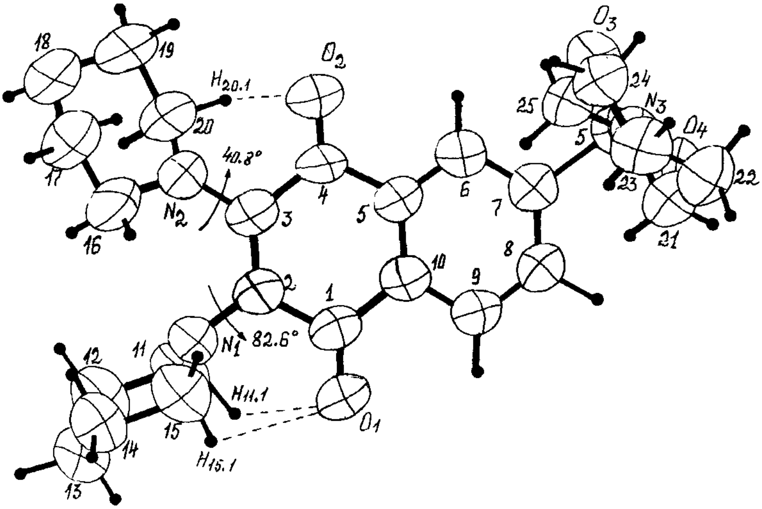

FIGURE 3 A general view of molecule III.

The N^2 lone electrone pair (LEP) is directed towards the carbonyl oxygen O^2 atom, while for the N^1 atom, to the opposite direction of the carbonyl O^1 atom. This character of mutual orientation of the piperidine substituents and the naphthoquinone fragment leads to a significant weakening of the ($n_N\pi^*$) interaction for the N^1 atom, as compared to N^2, that accounts for different bond lengths of N^2—C^3, 1.372(5) Å, and N^1—C^2, 1.420(5) Å.

Such a marked difference in the conformation of molecules III and II may be accounted for by the crystal packing influence. Modelling of the crystal environment of III in the crystal packing of II has shown that an oxygen atom replacement in the tosyl group of the morpholine fragment by a CH_2 group leads to an appearance of short C ··· H contacts of 2.3 ÷ 2.5 Å between the molecules in the stack. That should evidently result in changes both in the crystal and molecular structure of III as compared to II.

Just like in II, steric repulsions take place between the piperidine 2,3-substituents, which is confirmed by a short $C^{16} \cdots N^1$ contact 2.84 Å as well as by the nitrogen atoms N^1 (0.1 Å) and N^2 (−0.04 Å) deviating from the naphthoquinone plane to the opposite direction.

The conformation of the piperidine cycles is the same: "chair" with twist angles along the lines $C^{11} \cdots C^{15}$ and $C^{12} \cdots C^{14}$ by 49.3° and 55.2° (N^1-cycle) and along the lines $C^{16} \cdots C^{20}$ and $C^{17} \cdots C^{15}$ by 49.1° and 53.1° (N^2-cycle), respectively.

Similar to those in molecule II there are shortened contacts in III between the atoms O^1 and O^2 and $H^{11.1}$, $H^{20.1}$ and $H^{15.1}$ connected to the carbon atoms of the morpholine cycles: $O^1 \cdots H^{15.1}$ 2.57, $O^1 \cdots H^{11.1}$ 2.44 and $O^2 \cdots H^{20.1}$ 2.27 Å. The structure parameters calculated by Trotter (Table II), as in II, testify for an advantageous direction of the hydrogen atoms $H^{11.1}$, $H^{20.1}$ and $H^{15.1}$ on the p_Z-orbital of the carbonyl oxygen atoms O^1 and O^2, which points at a possibility of elimination of hydrogen atoms.

Bond lengths and bond angles in the piperidinosulfonyl substituent have ordinary values. Piperidine has a "chair" conformation with twist angles along the $C^{21} \cdots C^{25}$ and $C^{22} \cdots C^{24}$ lines by 50.0° and 55.1°, respectively. The N^3 nitrogen atom is 0.35 Å out of the coordination plane in the piperidine cycle.

In a crystal (Figure 4), molecules III as well as II form irregular stacks oriented along the "c" direction. Overlapping of molecules in the stack occurs between the naphthoquinone fragments. The pair IMIE in the stacks is −15.1 and −9.1 kcal/mol. The pair IMIE between the molecules of the neighbouring stacks related along the "c" direction with the screw axis 2_1 reaches −11.6 kcal/mol, i.e. comparable to the IMIE values in the stack, hence, the main structural element of the molecules III packing is a layer. The IMIE between the layers, equal to −2.2 kcal/mol, is determined by the interaction between the piperidine fragments.

3. Crystal Structure of Compound VI

The general view of molecule IV is shown in Figure 5. The naphthoquinone fragment in the molecule is mostly planar. The largest deviation from planarity is caused by a twist along the $C^3 \cdots C^5$ line by 11.0°, which leads to the carbonyl oxygen atom O^2 deviating the plane of the naphthoquinone fragment (−0.33 Å). Another carbonyl oxygen O^1 atom is 0.03 Å out of the same plane.

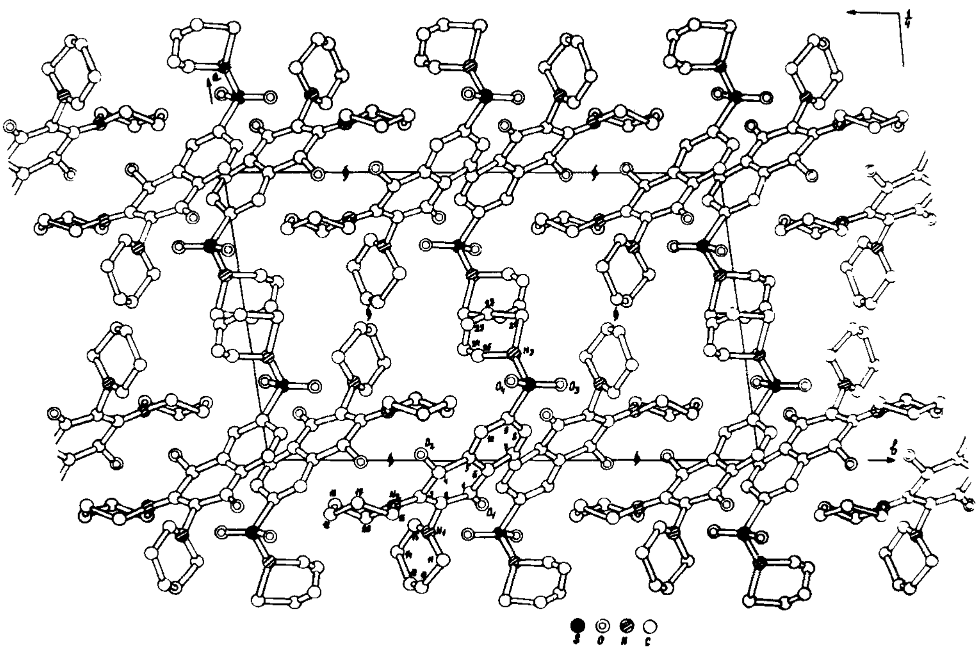

FIGURE 4 Projection of a crystal packing of molecules III on the XYO plane.

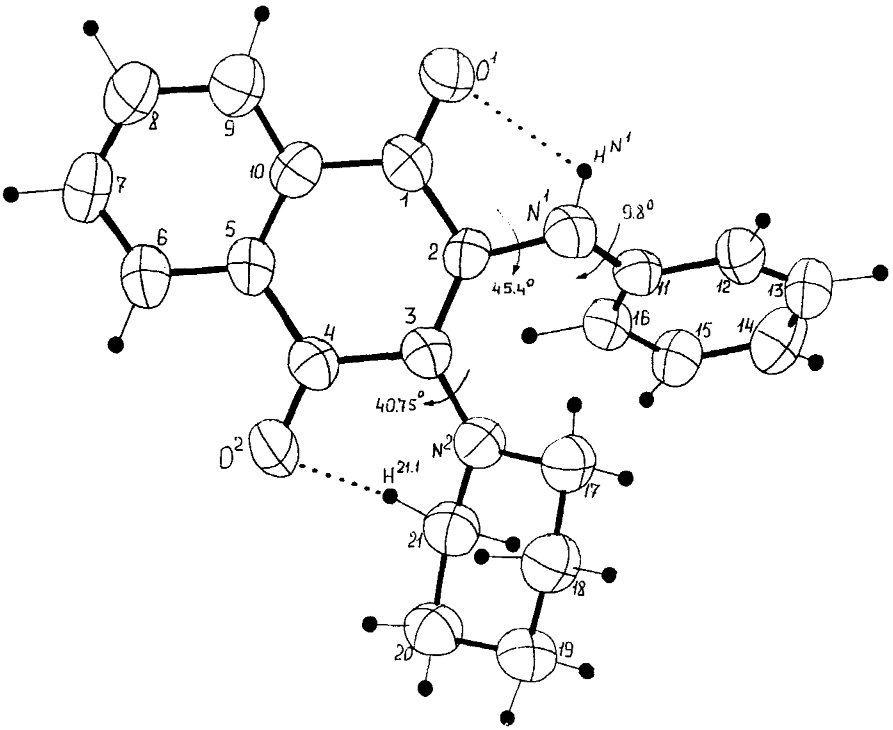

FIGURE 5 A general view of molecule IV.

The orientation of the aniline substituent with respect to the naphthoquinone fragment is characterized by dihedral angles between the naphthoquinone plane and the coordination N^1 atom plane, 45.4°, as well as between the phenyl ring plane and the coordination N^1 atom plane, 9.8°. The nitrogen N^1 atom has a pyramidal coordination and is 0.18 Å out of the coordination plane, while the lone N^1 pair is pointed to the opposite direction of the carbonyl oxygen O^1 atom. An analysis of distances $N^1 \cdots O^1$ 2.61 Å and $H_{N^1} \cdots O^1$ 2.21 Å and angles $C^1O^2H_{N^1}$ 81.0° and $O^1H_{N^1}N^1$ 113.0° allows us to conclude that there is an intramolecular hydrogen bond (IHB) $= O \cdots H{-}N\langle$.

The dihedral angle between the piperidine fragment N^2 atom coordination plane and the naphthoquinone fragment plane is 40.8°. The nitrogen N^2 atom in this substituent has a planar-trigonal coordination and, probably, due to a stronger $(n_N\pi^*)$-interaction the $C^3{-}N^2$ bond length (1.358(3) Å) is shorter than the $C^2{-}N^1$ one (1.398(3) Å). The piperidine substituent has a "chair" conformation with a twist along the $C^{17} \cdots C^{21}$ and $C^{18} \cdots C^{20}$ lines by 52.1° and 50.3°, respectively. As in II–III, the arising short contacts between the atoms of 2,3-substituents ($C^{17} \cdots C^{11}$ 3.08 and $C^{17} \cdots N^1$ 3.03 Å) prevent the tendency to greater planarity of the molecule.

Similar to compounds II–III, there is formed a shortened contact $H^{21.1} \cdots O^2$ (0.38 Å) and $C^4O^2H^{21.1}$ (85.3°) in IV. Atom $H^{21.1}$ deviates out of the (O^2, C^4 and C^3) plane by 1.6 Å. The Trotter structural parameters (Table II) also testify for the possibility of the $H^{21.1}$ hydrogen atom elimination.

Crystal packing IV is shown in Figure 6. Translationally related molecules IV

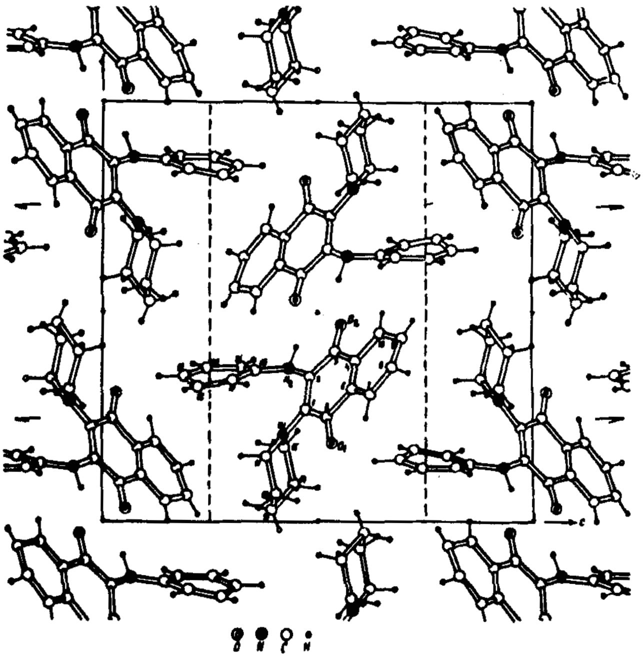

FIGURE 6 Projection of a crystal packing of molecules IV on the YZO plane.

form a stack packing in the direction of an "a" short period with a maximal value of IMIE in the crystal of −9.5 kcal/mol. The IMIE between the centro-symmetric molecule pairs is almost the same, −9.4 kcal/mol. The following level of molecular arrangement is determined by a pair interaction between the molecules related by a glide plane (−5.8 kcal/mol). Hence, the molecule IV packing is close to isotropic.

4. The Study of Photochemical Transformations of Compounds II–IV in Solution

We have studied photochemical transformations in solution for all the studied II–IV compounds. The solution of the studied compound in ethanol was irradiated with full UV-light. The photochemical transformations were analyzed against electron absorption spectra in UV- and visible region.

The form of spectra for compounds II and III is qualitatively identical (Figures 7a and 8a). The presence of three isobestic points in these spectra should be

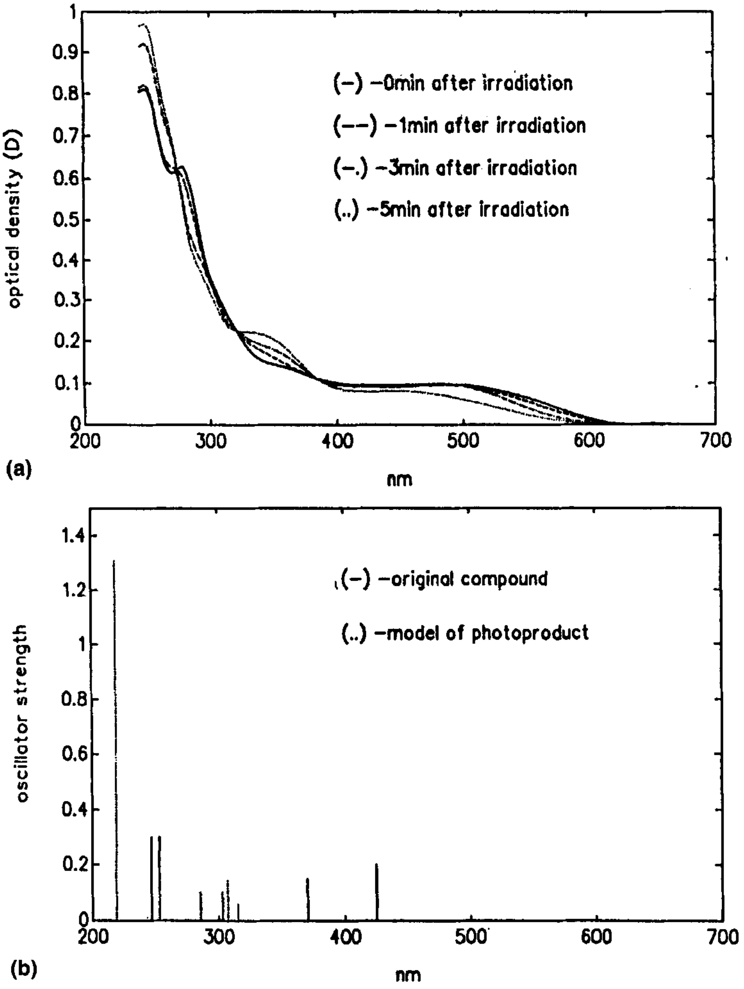

FIGURE 7 Experimental (a) and theoretical (b) absorption spectra of compound II in ethanol.

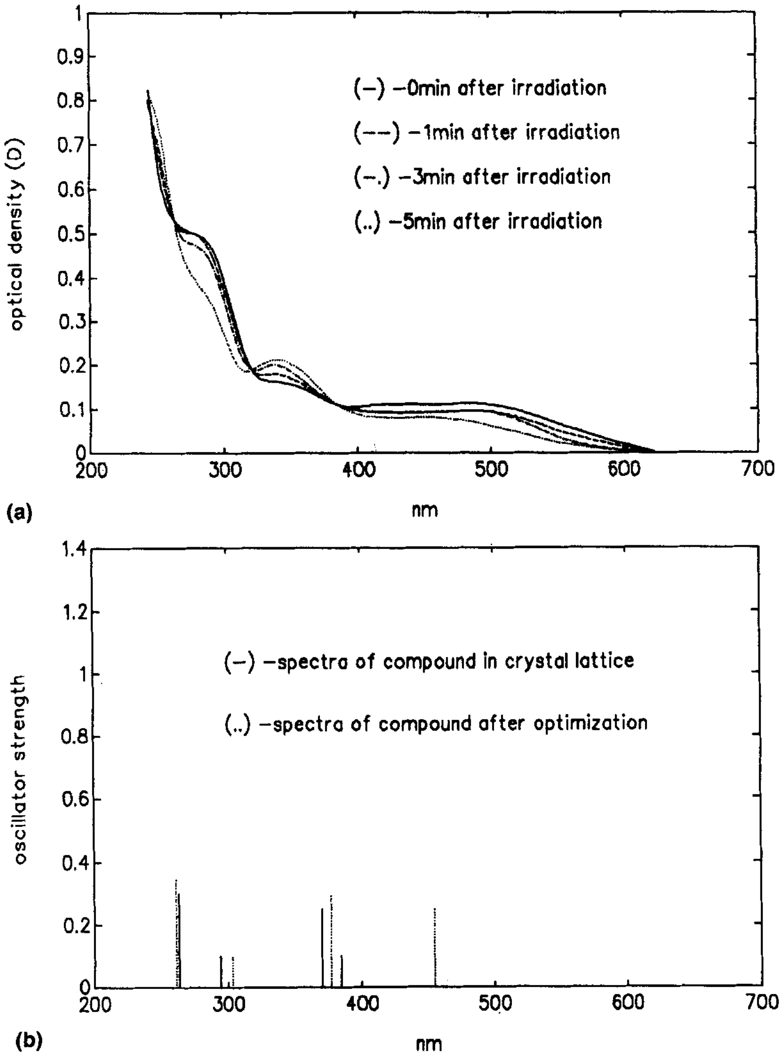

FIGURE 8 Experimental (a) and theoretical (b) absorption spectra of compound III in ethanol.

mentioned. This testifies for the fact that the solution in this spectral region is two-component,[6] i.e. a monomolecular reaction $A \xrightarrow{h\nu} B$ takes place under UV-irradiation. Using quantum-chemical calculations performed for II and III by the INDO/S method their theoretical spectra have been built (Figures 7 and 8b) and identification of the bands for each of the compounds studied made.

The position of absorption bands in the theoretical spectrum of II (Figure 7b) satisfactorily agrees with the experimental one (Figure 7a). From the electron density redistribution at $S_0 \rightarrow S_1$ transtion (Figure 10a) it follows that the long-wave band in the absorption spectrum corresponds to a $(l - \pi^*)$ electron transition.[7] Appearance of this band is evidently due to the electron density transfer from p_Z

atomic orbitals of the N^1 and N^2 nitrogen atoms to a π^*-antibonding orbital of the naphthoquinone fragment. Thus the intensity of this transition reflects the degree of the molecule planarity in solution.

The following three electron transitions have a (n-π^*) character, i.e. an electron transition takes place between the p_X and p_Y atomic orbitals of the O^1, O^2, N^1 and N^2 atoms and the orthogonal to them π^*-antibonding naphthoquinone orbital.[7] In the second and fourth transitions (~345 and ~250 nm) the electron density is transferred mainly from the p_X and p_Y atomic orbitals of both the carbonyl oxygen atoms O^1, O^2 and the nitrogen atoms N^1 and N^2 to the π^*-antibonding orbital of the naphthoquinone. And for the third absorption band (~294 nm) the (n-π^*) transition takes place only from the LEP of the carbonyl oxygen atoms O^1 and O^2 to the $\pi^*_{C=O}$-antibonding orbital.

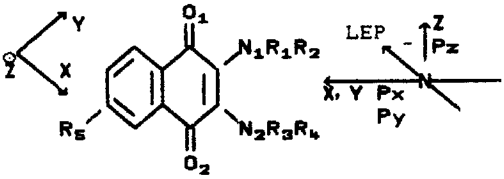

The theoretical spectrum of compound III calculated using the crystallographic coordinates (Figure 8b) differs from the experimental one (Figure 8a) in the absence of a pronounced long-wave band, besides, there occurs an inversion of (n − π^*) and (l − π^*) transitions (Figure 10b). It may be connected with the difference in the conformations of molecules II and III, caused, as is shown above, by the influence of the intermolecular interactions (IMI) in the crystal. In II, the rotation of the morpholine substituents around the C—N bonds are equal to 44 ÷ 45°, while in III, the rotation of the piperidine substituents are different: ~45° and ~90°. In solution, the molecule, when IMI are absent, can have a different conformation. The similarity of the theoretical spectrum of the molecule II and the experimental spectrum of III in solution testifies for the fact that this molecule in solution has a more planar conformation. To confirm the suggestion we have performed a calculation of the model structure theoretical spectrum with rotational angles around C—N bonds analogous to those in II. A sufficiently good agreement of the theoretical band position with the experimental one has been obtained (Figure 8b). The nature of the observed electron transitions in the model molecule III has appeared to be identical to that in II.

The experimental absorption spectrum of compound IV in solution differs from those of II and III by the absence of the isobestic points, i.e. the system is more than two-component (Figure 9a). There appears a long-wave absorption band in the range of ~625 nm that is characteristic of an absorption band of ions or radicals. The theoretical spectrum of compound IV (Figure 9b) has no long-wave absorption band found in the experiment. However, an analysis of the crystal packing testifies for the absence of any significant intermolecular interactions capable of changing considerably the molecule conformation in crystal as compared to solution. At the same time, compound IV is more planar due to IHB as compared to II and III, that leading to higher aromaticity, hence, to higher stability of the molecular struc-

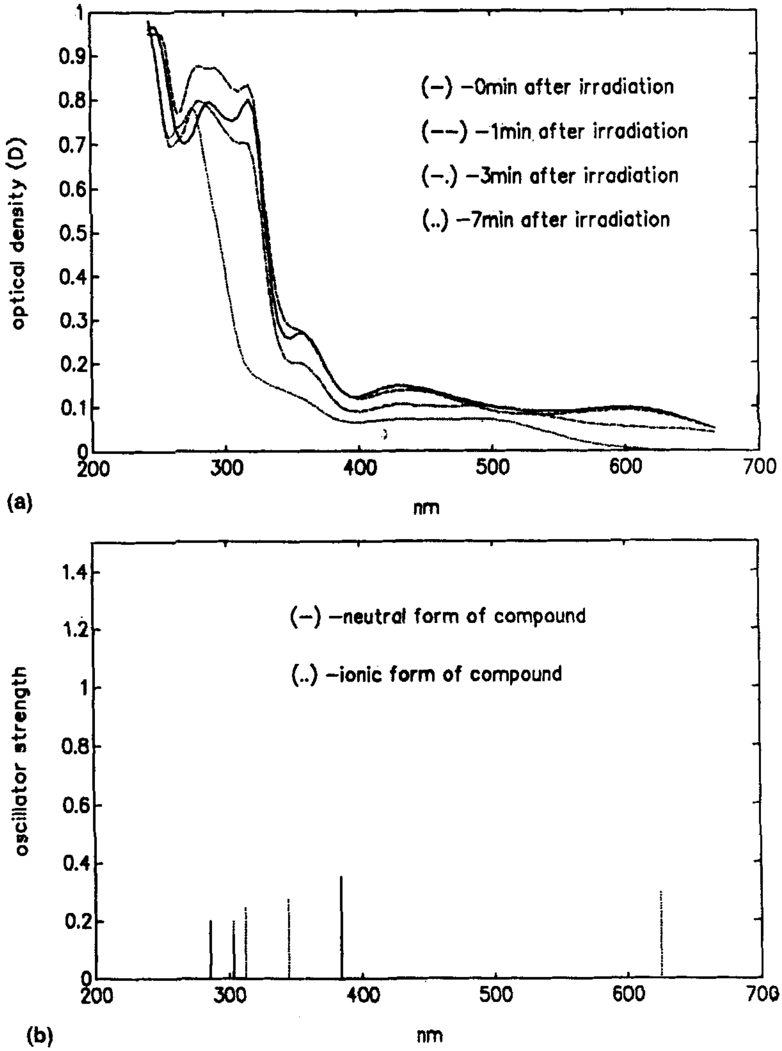

FIGURE 9 Experimental (a) and theoretical (b) absorption spectra of compound IV in ethanol.

ture to conformational changes. That can be explained by the fact that in solution we have an equilibrium of two forms *A* and *B* (Scheme III), where *A* is the initial molecule and *B* is the zwitterionic form arising due to an intramolecular proton transfer. The calculation of the theoretical zwitterionic *B* form spectrum together with the initial *A* form (Figure 9b) allows one to reach a satisfactory agreement between the theoretical and experimental data. All electronic transitions for form *B*, as well as the long-wave transition for *A* (~385 nm) belong to the (l – π^*) type (Figure 10c). The remaining transition of form *A* belongs to the (n – π^*) (~311 and ~286 nm) types.

Analysis of the absorption spectra under UV-irradiation shows the identical behavior of compounds II and III in solution. Under irradiation, an intensity drop

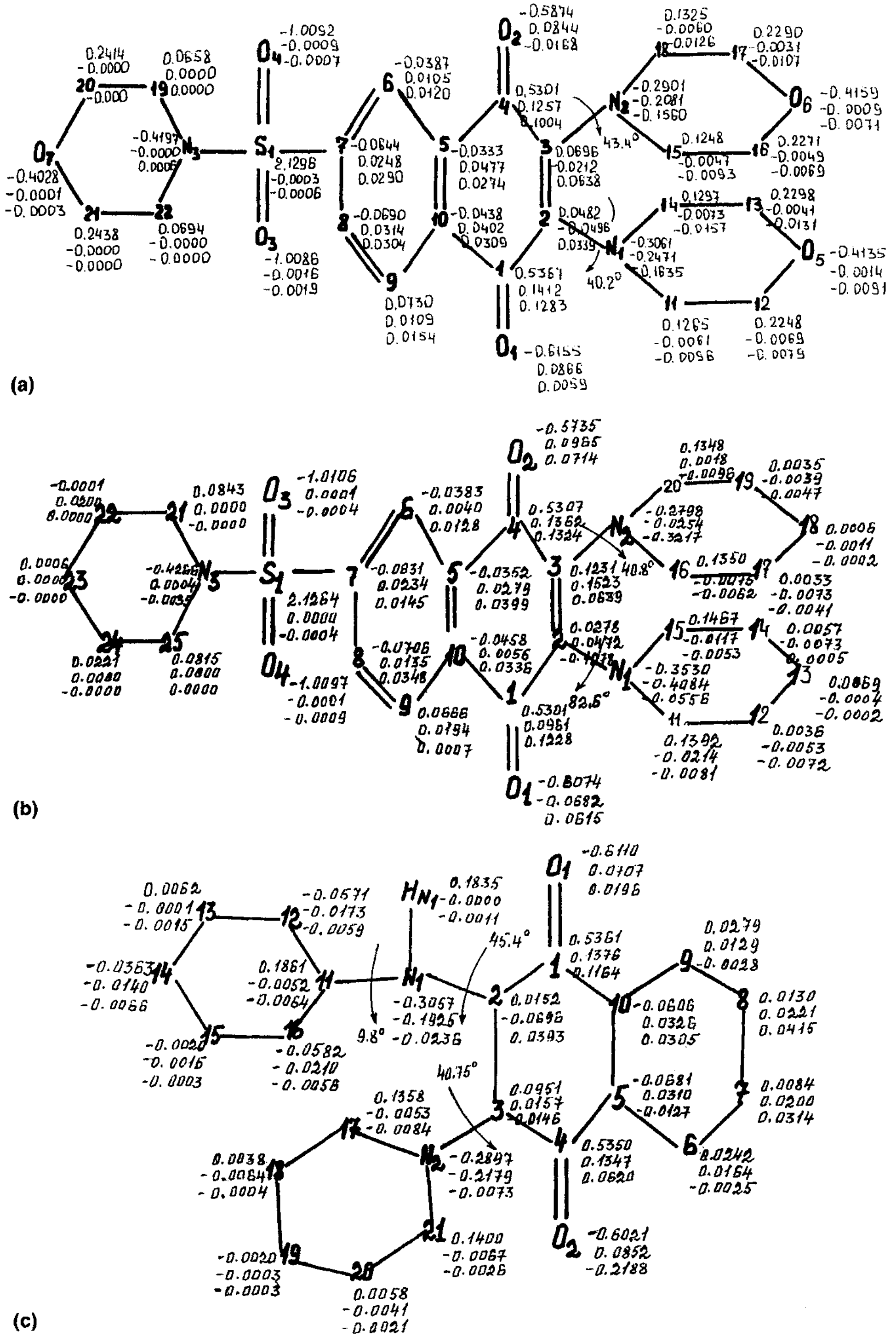

FIGURE 10 Redistribution of electron density at the $S_0 \rightarrow S_1$ and $S_0 \rightarrow S_2$ transitions in the molecule II (a), III (b) and IV (c). In the numerator—atomic charge in ground state and in the denominator—change of atomic charges in the first and second singlet excited states.

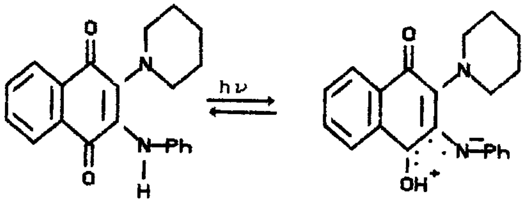

SCHEME III

in the spectra of these compounds takes place for the long-wave (l – π^*) transitions and for the (n – π^*) transitions localized mainly on the atoms of the carbonyl group. An intensity increase is observed for the (n – π^*) transitions. These variations point to the conversion of the carbonyl group double bond into a single one, as well as to the absence of conjugation between the nitrogen atoms LEP with a π-system of the naphthoquinone fragment in the photoproduct as compared to the initial molecule.

The above-mentioned analysis of the structural parameters in Table IV according to Trotter[2–4] together with the data on electronic spectroscopy testifies for a possibility of a hydrogen atom elimination by a carbonyl oxygen atom for the (l – π^*) transition. This is due to the structure of the compounds studied where the hydrogen atom is directed just to the p_Z-orbital localized on the carbonyl group atoms.

Then, by analogy with the literature data[1] a mechanism of synchronous cycle closure (Scheme IV) with 2H˙ elimination has been suggested. In the photoproduct suggested the double bond of the carbonyl group, as is assumed, becomes a single one, and the nitrogen atom, according to evaluation by molecular mechanics technique[8], becomes essentially pyramidal. Atoms N are ~0.3 Å out of the coordination plane, which leads to a decreased conjugation of the LEP of N with the naphthalene fragment π-system and, hence, to a transformation of a (l – π^*) transition into (n – π^*). This character of photoreaction testifies also for a similarity of the photoproduct theoretical spectrum and the experimental spectrum of II–III after UV-irradiation (Figure 7b).

For compound IV under UV-irradiation there is observed an intensity drop for the (l – π^*) transition (~635 nm) of the assumed ionic form *B*, while the band intensities in the spectral region (313 and 300 nm) increase. On further irradiation the spectrum of IV becomes identical to the spectra of the nonirradiated compounds (II–III). This testifies evidently for the fact, that under UV-irradiation in solution the proton phototransfer reaction mainly takes place (Scheme III), but in this case there are no isobestic points in the spectrum. It may be explained, probably, by a participation of the ethanol molecule of the proton donor in the photoprocess.

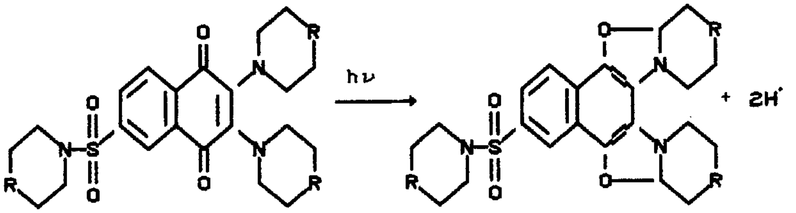

SCHEME IV

5. Theoretical Simulation of Photoreaction

For a more detailed analysis of the process we have made a comparison of the electronic part of the interatomic interaction energy in the compounds studied for the ground and excited states at the (l − π^*) transition. The calculation has been performed based on the data on energy decomposition. The main idea of the technique is using the Hartree-Fock-Roothaan equation for electronic energy E:

$$E = \sum_i \sum_j P_{ij}[H_{ij} + F_{ij}]/2 = \sum_i \sum_j E_{ij}^{AO}$$

where P_{ij} is the density matrix, H_{ij} is the core matrix (an influence of non-valent electrons and an electron-nuclear interaction), F is the Fock matrix (electron-electron interaction) and E_{ij}^{AO} is the pair electronic energy between the atomic orbitals.

Here

$$P_{ij} = 2^* \sum_k^{N/2} C_{ik}C_{jk}; \qquad \Psi_i = \sum C_{ik}\Phi_k$$

where Ψ_i is the molecular orbital, Φ_k is the atomic orbital and C_{ik} is the probability amplitude of the Ψ_i localization on Ψ_k. The matrix elements F, H and P for the calculation are taken from the semiempirical method MNDO.[9]

Further on we have carried out summation of E_{ij}^{AO} to which correspond the atomic orbitals localized on the pairwise different atoms. Thus we have obtained the partial energy components of the atom-atomic interactions. Because of the program limitations the calculations have been carried out on a model molecule (Figures 11a–c).

The calculations for the model molecule for compounds II and III in solution show (Figure 11a) that at the $S_0 \rightarrow S_1$ (l − π^*) transition the $\rangle C^2{=}C^3\langle$ bond becomes much more antibonding. This increase of antibonding is reflected in a decrease by ~1.8 ev of the interaction electron energy. The repulsion between atoms $C^2 \cdots N^2$, $C^3 \cdots N^1$ and $N^1 \cdots N^2$ increases by 0.23, 0.21 and 0.04 ev, respectively, which can be explained mainly by the repulsions of the π-orbitals of these atoms. Based on these calculations it may be concluded that when the molecule is excited the nitrogen atoms are pushed towards the carbonyl groups. In its turn that leads to shortening of the contact between the oxygen carbonyl atoms and the carbon atoms in the piperidine or morpholine cycles. All this will enhance the proposed cyclization (Scheme IV).

For the neutral form A of the compound IV in solution the results of the calculation for the (l − π^*) transition were the same as for II and III with the only difference that there was an additional antibonding of the N—H bond by 0.06 ev and an attractive interaction $=O \cdots H{-}N\langle$ increased by 0.01 ev (Figure 11b). Therefore, the acidity of the hydrogen atom increased. Hence, for the relaxation of the molecule structure similar to II and III, in the excited state the shortened contacts $=O \cdots H{-}C\langle$ and $=O \cdots H{-}N\langle$ would rather lead to an intramolecular

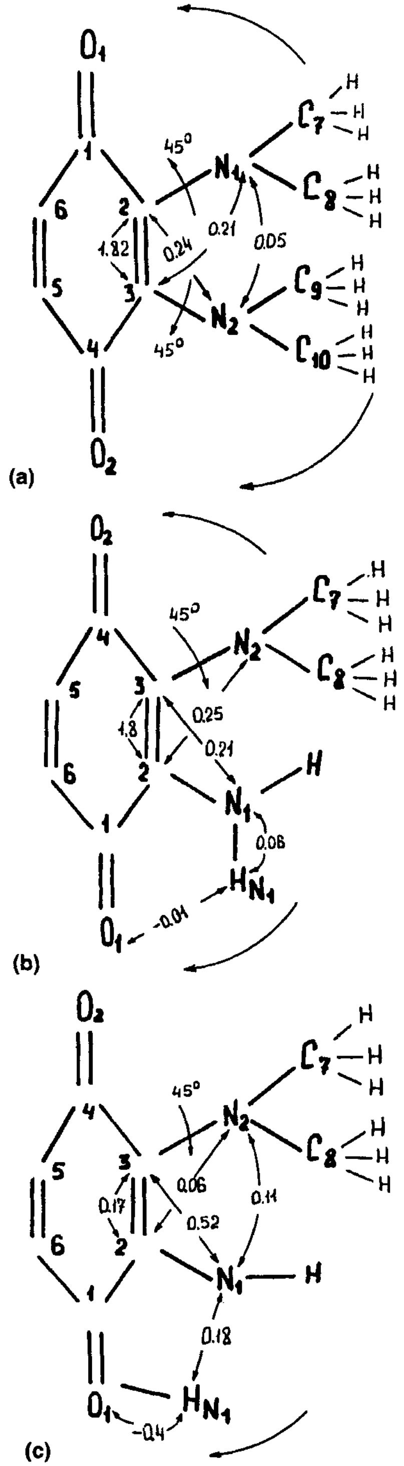

FIGURE 11 Changes in the electronic energy of atom-atomic interaction at the $S_0 \rightarrow S_1$ transition for the model molecules II and III (a); for the neutral form *A* of the model molecule IV (b) and for the zwitterionic form *B* of the model molecule IV (c).

proton transfer to give an ionic *B* form than to a homolytic rupture of the C—H bond followed by cyclization.

An analysis of the changes taking place at the $S_0 \rightarrow S_1$ transition in the ionic *B* form of the compound IV (Figure 11c) shows that a marked increase of the repulsion $C^3 \cdots N^1$ (0.52 ev) against the background of an insignificant increase of the repulsion $C^2 \cdots N^2$ (0.058 ev) and $N^1 \cdots N^2$ (0.1 ev) enhances a reverse proton transfer. Thus in IV the process of photocyclization is hindered by a reversible proton phototransfer.

The preliminary data on the photochemistry of compounds II and III in the solid phase testify for the fact that the same photoconversion takes place in crystal.

Acknowledgment

We are grateful to V. M. Anisimov for useful and critical discussion on the interpretation of the quantum-chemical calculation results.

References

1. E. P. Fokin and E. P. Prudchenko, *Izvestija SO AN SSSR*, N7. vy p. 2. 1966, s. 98.
2. J. Trotter, *Acta Cryst.*, **B39**, N3, 373–381 (1983).
3. W. K. Appel, Z. Q. Jiang, J. R. Scheffer and L. Walsh, *J. Am. Chem. Soc.*, **105**, N16, 5354–5363 (1983).
4. S. Ariel, S. Askaki and J. R. Scheffer *et al.*, *J. Am. Chem. Soc.*, **104**, N19, 5726–5728 (1984).
5. G. V. Timofeeva, N. J. Chernikova and P. M. Zorkii, *Uspekhi Khimii*, **69**, 966 (1980).
6. I. Ja. Bernshtein and Ju. L. Kainskii, *Spectrofotometricheskii analiz v organicheskoi khimiji*, Khimija, 1975.
7. O. V. Sverdlova, *Electronnye spectry v organicheskoi khimii*, Khimija, 1985.
8. N. L. Allinger and Y. Yuh, *Molecular Mechanics*. MM2 and MMP2 programs. October, 1977.
9. Modified Neglect of Diatomic Difference Overlap SCF MO. Version 2.07, Universidad de La Habana, 1987–1989.